

# Inorganic Excimer. Spectroscopy, Photoredox Properties and Excimeric Emission of Dicyano(4,4'-di-*tert*-butyl-2,2'-bipyridine)platinum(II)

Kam-To Wan,<sup>a</sup> Chi-Ming Che<sup>\*,a</sup> and Kar-Cheong Cho<sup>b</sup>

<sup>a</sup> Department of Chemistry, University of Hong Kong, Pokfulam Road, Hong Kong

<sup>b</sup> Department of Physics, The Chinese University of Hong Kong, Shatin, New Territories, Hong Kong

The complex  $[\text{Pt}(\text{dtbipy})(\text{CN})_2]$  (dtbipy = 4,4'-di-*tert*-butyl-2,2'-bipyridine) has a long-lived intra-ligand ( $\pi\pi^*$ )<sup>3</sup> excited state in fluid solutions (room-temperature lifetime at infinite dilution 3  $\mu\text{s}$  in 1,2-dichloroethane). Excimer emission (maximum 565 nm) and photoinduced oligomerisation have been found for this platinum complex. The measured rate constant for the process  $[\text{Pt}(\text{dtbipy})(\text{CN})_2]^* + [\text{Pt}(\text{dtbipy})(\text{CN})_2] \longrightarrow \{[\text{Pt}(\text{dtbipy})(\text{CN})_2]_2\}^*$  is  $9.0 \times 10^8 \text{ dm}^3 \text{ mol}^{-1} \text{ s}^{-1}$  in 1,2-dichloroethane at room temperature. The photophysics and photoredox properties of the excited monomer and dimer are discussed.

Few examples of inorganic systems are known to exhibit excimer emission, a phenomenon which is usually encountered in the photochemistry of aromatic molecules. In the course of our studies on metal  $d^8$ - $d^8$  interactions we have found that square-planar platinum(II) complexes such as  $[\text{Pt}(\text{bipy})(\text{CN})_2]$  (bipy = 2,2'-bipyridine) and  $[\text{Pt}(\text{phen})(\text{CN})_2]$  (phen = 1,10-phenanthroline) display intense photoluminescence in the solid state,<sup>1</sup> the emission maxima of which are very sensitive to solid-state effects. In a recent report by Miskowski and Houlding<sup>2a</sup> such observation has been attributed to ligand-ligand excimeric interaction in the solid state, which could perturb the emission properties of the platinum(II) complexes. A simplified molecular-orbital diagram for the platinum(II)-diimine system, taking into account this type of interaction, is shown in Fig. 1. In order to gain insight into the relative importance of ligand-ligand and metal-metal interactions occurring in one-dimensional platinum(II) systems, we have synthesised dicyano(4,4'-di-*tert*-butyl-2,2'-bipyridine)platinum(II)  $[\text{Pt}(\text{dtbipy})(\text{CN})_2]$  as the model compound for the study. This compound was chosen because of its high solubility in non-polar solvents. Since the completion of this work, Kunkely and Vogler<sup>2b</sup> have reported excimer formation and luminescence from the related complex dicyano(4,7-diphenyl-1,10-phenanthroline)platinum(II).

## Experimental

**Materials.**—The ligand 4,4'-di-*tert*-butyl-2,2'-bipyridine (dtbipy)<sup>3a</sup> and  $\text{Pt}(\text{CN})_2 \cdot x\text{H}_2\text{O}$ <sup>3b</sup> were prepared by the literature methods. All organic quenchers for photochemical studies were purified by repeated recrystallisations or distillation. The complex  $[\text{Pt}(\text{dtbipy})(\text{CN})_2]$  was prepared by refluxing  $\text{Pt}(\text{CN})_2 \cdot x\text{H}_2\text{O}$  (0.24 g) and dtbipy (0.23 g) in dimethylformamide (50  $\text{cm}^3$ ) for 8 h. After refluxing, the solution was filtered. The pale green solid was washed several times with diethyl ether and recrystallised by vapour diffusion of diethyl ether into acetonitrile. Yield 80% {Found: C, 46.7; H, 4.6; N, 10.7. Calc. for  $[\text{Pt}(\text{dtbipy})(\text{CN})_2]$ : C, 46.6; H, 4.7; N, 10.9%}. IR:  $\nu(\text{CN})$  2148.3 and 2136.9  $\text{cm}^{-1}$ .

**Physical Measurements.**—Ultraviolet/visible absorption spectra were obtained on a Shimadzu UV-240 spectrophotometer, steady-state emission and excitation spectra with or without Corning filters on a Hitachi 650-60 fluorescence

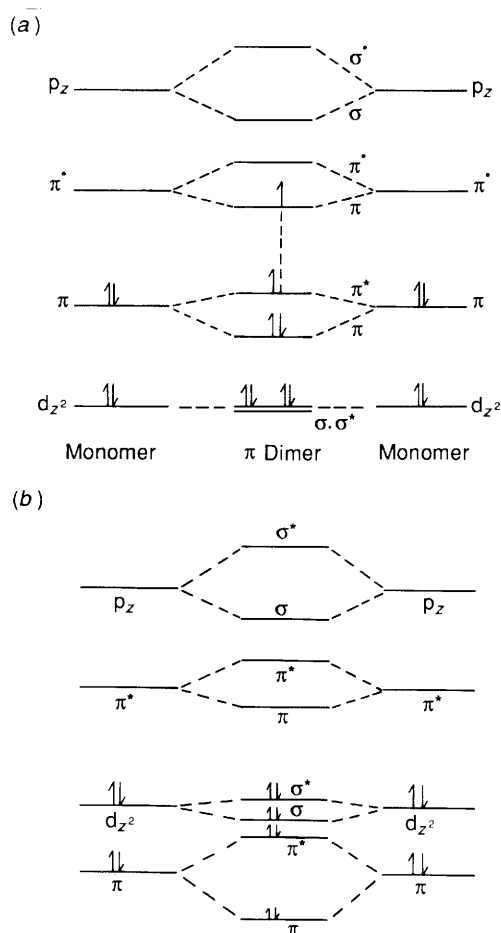


Fig. 1 Simplified molecular-orbital diagram for  $[\text{Pt}(\text{diimine})(\text{CN})_2]$ : (a) energy of  $\pi$ - $\pi^*$  excimer is higher than that of  $d_{z^2}$  excimer (ref. 2); (b) energies of  $\pi$ - $\pi^*$  and  $d_{z^2}$  excimers are similar

spectrophotometer. Self-quenching phenomena were investigated by the Stern-Volmer quenching method. The sample was degassed by at least four freeze-pump-thaw cycles. Linear plots of reciprocal lifetime *versus* complex concentration were obtained, from which the self-quenching rate constant and

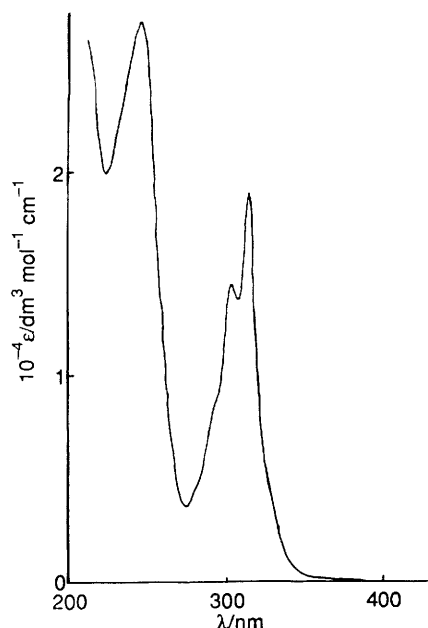


Fig. 2 Ultraviolet/visible absorption spectrum of  $[\text{Pt}(\text{dtbbpy})(\text{CN})_2]$  in acetonitrile

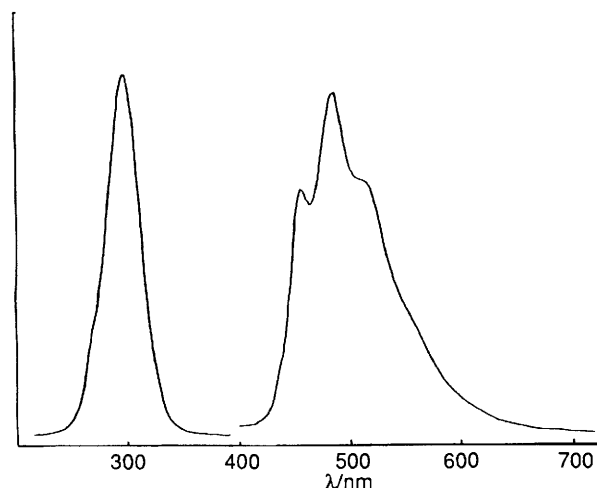


Fig. 3 Emission and excitation spectra of  $[\text{Pt}(\text{dtbbpy})(\text{CN})_2]$  ( $10^{-5}$  mol  $\text{cm}^{-3}$ ) in acetonitrile

lifetime at infinite dilution ( $\tau_0$ ) were deduced. For lifetime measurements, the excitation source was the 355 nm output of a Quanta-Ray Q-switched DCR-3 pulsed Nd:YAG laser. The laser energy was set at about 3 mJ per pulse to avoid photodecomposition of the metal complex.

### Results and Discussion

The platinum complex was prepared by the reported method for  $[\text{Pt}(\text{bipy})(\text{CN})_2]$  whose structure has been established by X-ray crystallography.<sup>1</sup> As expected, the present complex displays two  $\nu(\text{CN})$  stretches, in accordance with a *cis* geometry. Its electronic absorption spectrum (Fig. 2) is characterised by an intense vibronic structured band (maximum at 315 nm), which is assigned to the lowest-energy spin-allowed intraligand  $\pi \rightarrow \pi^*$  transition of dtbbpy. There is also an intense absorption band at 240–250 nm, but the nature of the transition is uncertain. However, the UV/VIS absorption spectra of both  $[\text{Ir}(\text{bipy})_3]^{3+}$  (refs. 4 and 5) and  $[\text{Rh}(\text{phen})_3]^{3+}$  (ref. 5) also show similar bands at similar energies. In Fig. 2 it is also possible that a low-lying metal-to-ligand charge-transfer (m.l.c.t.) state  $\text{Pt} \rightarrow \pi^*(\text{dtbbpy})$  lies underneath the tail of the  $\pi \rightarrow \pi^*$  transition. The occurrence of such a state at

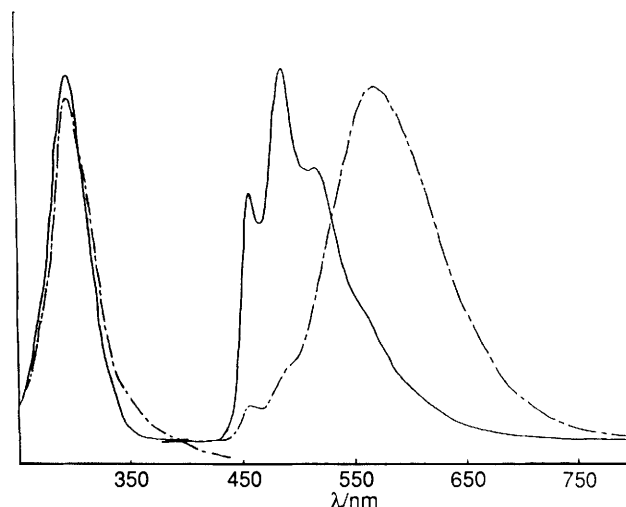
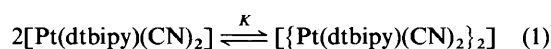


Fig. 4 Emission and excitation spectra of  $[\text{Pt}(\text{dtbbpy})(\text{CN})_2]$  ( $\cdots$ ),  $2 \times 10^{-3}$ ; —,  $9.8 \times 10^{-6}$  mol  $\text{dm}^{-3}$ ) in 1,2-dichloroethane

around 330–380 nm is not unreasonable since  $\text{Pt}^{\text{II}}$  should have higher m.l.c.t. energy than its  $\text{Rh}^{\text{I}}$  analogue,<sup>6,7</sup> and the  $d_{z^2}(\text{Rh}) \rightarrow \pi^*(\text{bipy})$  transition for  $[\text{Rh}(\text{bipy})_2]^+$  occurs at 505 nm.<sup>8</sup>

Room-temperature photoluminescence has been observed; the emission and excitation spectra in acetonitrile measured under high dilution conditions ( $[\text{complex}] = 10^{-6}$ – $10^{-5}$  mol  $\text{dm}^{-3}$ ) are shown in Fig. 3. The emission spectrum is independent of the excitation wavelength from 300 to 350 nm. A similar emission spectrum has been recorded in dichloromethane. The emission arises from the intraligand ( $\pi\pi^*$ ) triplet because of its long lifetime (room-temperature lifetime at infinite dilution is 3  $\mu\text{s}$  in dichloromethane). The observed smaller vibronic spacing of 1100–1200  $\text{cm}^{-1}$  in the absorption spectrum than that of 1300–1400  $\text{cm}^{-1}$  in the emission spectrum is normally expected for the ( $\pi\pi^*$ )<sup>3</sup> state of aromatic diimines.

At concentrations of  $10^{-4}$ – $10^{-3}$  mol  $\text{dm}^{-3}$  in non-polar solvents such as 1,2-dichloroethane some ground-state association of  $[\text{Pt}(\text{dtbbpy})(\text{CN})_2]$  has been observed. Under these conditions, the absorbance at 360–410 nm does not follow Beer's law. By fitting the absorbance data at wavelengths 375, 380 and 385 nm, the equilibrium (1) has been found. The



equilibrium constant  $K$  should be small because there is no build up of a distinct new absorption band of the dimer at 360–500 nm even at complex concentrations up to  $7 \times 10^{-3}$  mol  $\text{dm}^{-3}$ .

Unlike the absorption spectrum, the emission spectrum of  $[\text{Pt}(\text{dtbbpy})(\text{CN})_2]$  in halogenocarbons is strongly affected by its concentration. At  $10^{-4}$ – $10^{-3}$  mol  $\text{dm}^{-3}$  in 1,2-dichloroethane, the emission is red-shifted to 565 nm (Fig. 4), the excitation spectrum (Fig. 4) being the same as that for the emission shown in Fig. 3. This indicates that ground-state dimerisation, as described above, is not responsible for the change in photoluminescence behaviour. Instead, the occurrence of excimeric emission is suggested. In accordance with this suggestion, the monomer emission decay as monitored at 485 nm follows a simple exponential over a very large range of complex concentration ( $10^{-6}$ – $10^{-3}$  mol  $\text{dm}^{-3}$ ) with the rate constant increasing linearly with sample concentration. In contrast, the emission at 565 nm, attributed to that of the excimer, does not reach its maximum until a certain time after the laser flash (see Fig. 5). This rise time (100 ns) is only weakly dependent on the sample concentration. At longer times, the excimer signal decays over a time-scale and fashion almost

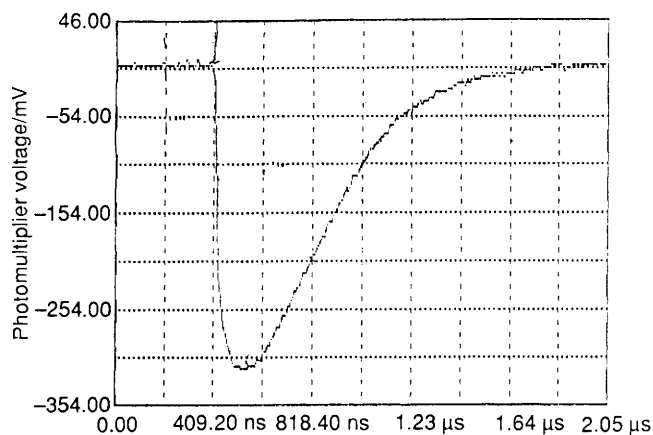


Fig. 5 Formation and decay of the emission signal of  $[\text{Pt}(\text{dtbipy})(\text{CN})_2]_2^*$  ( $4 \times 10^{-3}$  mol  $\text{dm}^{-3}$  Pt) monitored at 565 nm in 1,2-dichloroethane

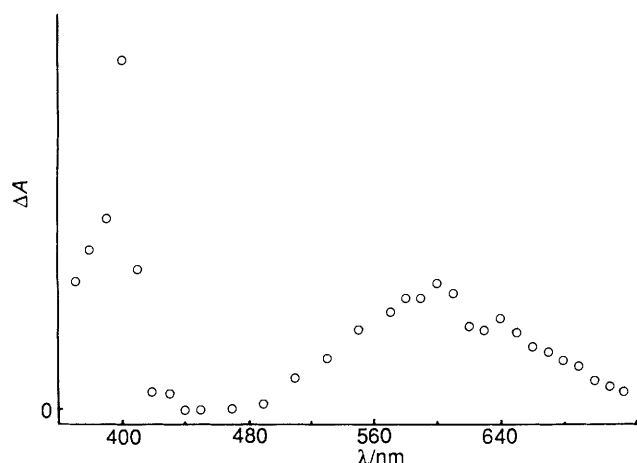
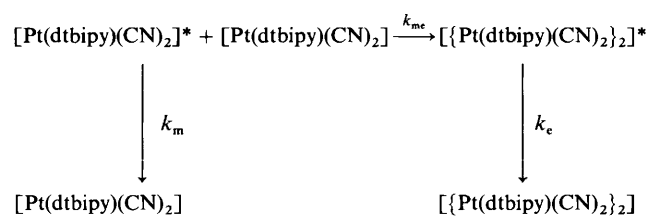


Fig. 6 Transient difference absorption spectrum recorded 10  $\mu\text{s}$  after flashing a degassed acetonitrile solution of  $[\text{Pt}(\text{dtbipy})(\text{CN})_2]$  and methyl viologen at 355 nm and at 20  $^\circ\text{C}$

identical to that of the monomer (Fig. 5). The above kinetic features suggest that the monomer–excimer kinetics can be described by Scheme 1.



**Scheme 1**  $[\text{Pt}(\text{dtbipy})(\text{CN})_2]^* = A_1 \exp\{-k_{\text{m}} + k_{\text{me}}[\text{Pt}(\text{dtbipy})(\text{CN})_2]\}_t$ ,  $[\{\text{Pt}(\text{dtbipy})(\text{CN})_2\}_2]^* = A_2 [\exp\{-k_{\text{m}} + k_{\text{me}}[\text{Pt}(\text{dtbipy})(\text{CN})_2]\}_t - \exp(-kt)]$

Two of the rate constants in Scheme 1,  $k_{\text{m}}$  and  $k_{\text{me}}$  can readily be obtained from the monomer quenching study as  $3.4 \times 10^5$   $\text{s}^{-1}$  and  $9.0 \times 10^8$   $\text{dm}^3 \text{mol}^{-1} \text{s}^{-1}$  in 1,2-dichloroethane and at room temperature, respectively. By fitting the excimer kinetics at 565 nm, the excimer decay rate constant  $k_{\text{e}}$  is deduced to be  $2.5 \times 10^7$   $\text{s}^{-1}$ . Because of this relatively high value, the decay of both the monomer and excimer are governed by the rate of excimer formation, thus accounting for the nearly identical decay kinetics observed for the two species. Similar findings have also been obtained in  $\text{CHCl}_3$  and  $\text{CH}_2\text{Cl}_2$ . In acetonitrile no excimeric emission was observed even at complex concentrations of up to  $2 \times 10^{-3}$  mol  $\text{dm}^{-3}$ .

The above finding provides support to the previous sug-

gestion that the solid-state emission of platinum(II) diimine complexes arises from excimeric emission. The red shift in emission energy from  $[\text{Pt}(\text{dtbipy})(\text{CN})_2]^*$  to  $[\{\text{Pt}(\text{dtbipy})(\text{CN})_2\}_2]^*$  is in accordance with either an extended ligand–ligand or metal–metal interaction along the Pt–Pt axis. Previous work<sup>17</sup> showed that there is a dramatic difference in colour between the solid  $[\text{Pt}(\text{phen})(\text{CN})_2]$  (violet) and its isostructural and isoelectronic palladium analogue (pale yellow). This suggests that the lowest-energy dipole-allowed transition in the  $[\text{M}(\text{diimine})(\text{CN})_2]$  system ( $\text{M} = \text{Pd}$  or  $\text{Pt}$ ) is unlikely to be pure ligand centred but rather  $d_{z^2} \rightarrow (p_z, \pi^*)$  in origin. Although the X-ray crystal structure of  $[\text{Pt}(\text{dtbipy})(\text{CN})_2]$  has not been determined, the  $\text{Bu}^t$  groups should prohibit close intermolecular contact, thus disfavouring metal–metal interactions. It is possible that the true species responsible for the excimeric emission could be a mixture of the metal  $d_{z^2}$  and  $\pi$ – $\pi^*$  ligand-based excimers.

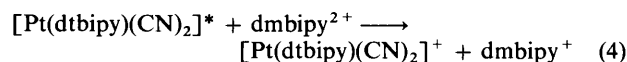
**Photochemical Reactivities of the  $\pi\pi^*$  Triplet of  $[\text{Pt}(\text{dtbipy})(\text{CN})_2]^*$ .**—The cyclic voltammogram of  $[\text{Pt}(\text{dtbipy})(\text{CN})_2]$  in acetonitrile exhibits a reversible one-electron reduction couple ( $\Delta E_{\text{p}} = 60$ – $70$  mV,  $i_{\text{p}}/i_{\text{p}} = 1$ ) at  $-1.2$  V and an irreversible anodic wave at 1.2 V (*vs.*  $\text{Ag} - \text{AgNO}_3$ ), which correspond to the ligand-centred reduction<sup>9</sup> and the metal-centred oxidation respectively. Since  $d^7$  monomeric platinum(III) species are expected to be unstable, it is not unreasonable to find that the oxidation wave is irreversible. From these electrochemical data, the excited-state potential can be estimated by equations (2) and (3). From the emission spectrum,  $E_{0-0}$  is estimated at 2.7 eV.

$$E^\circ(\text{Pt}^* - \text{Pt}^{\text{I}}) = E_{0-0} + E^\circ(\text{Pt}^{\text{II}} - \text{Pt}^{\text{I}}) \quad (2)$$

$$E^\circ(\text{Pt}^{\text{III}} - \text{Pt}^*) = E^\circ(\text{Pt}^{\text{III}} - \text{Pt}^{\text{II}}) - E_{0-0} \quad (3)$$

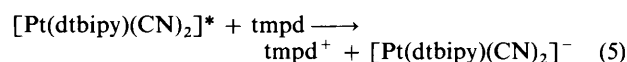
Thus  $[\text{Pt}(\text{dtbipy})(\text{CN})_2]^*$  is both a powerful oxidant and a powerful reductant, with  $E^\circ(\text{Pt}^* - \text{Pt}^{\text{I}})$  and  $E^\circ(\text{Pt}^{\text{III}} - \text{Pt}^*)$  at 2.1 and  $< -0.97$  V *vs.* normal hydrogen electrode respectively.

The ability of  $[\text{Pt}(\text{dtbipy})(\text{CN})_2]$  to perform bimolecular redox reactions has also been investigated. 1,1'-Dimethyl-4,4'-bipyridinium (methyl viologen),  $\text{dmbipy}^{2+}$ , has been found to quench its emission with a rate constant of  $2.0 \times 10^8$   $\text{dm}^3 \text{mol}^{-1} \text{s}^{-1}$ . Flash photolysis suggested that the quenching mechanism can be described by equation (4). Fig. 6 shows the



transient difference absorption spectrum, recorded 10  $\mu\text{s}$  after the laser flash, of a degassed acetonitrile solution of  $[\text{Pt}(\text{dtbipy})(\text{CN})_2]$  and  $\text{dmbipy}^{2+}$ . The spectrum is essentially the same as that of  $\text{dmbipy}^+$  ( $\lambda_{\text{max}}$  395 and 605 nm),<sup>10</sup> indicating that the oxidised species  $[\text{Pt}(\text{dtbipy})(\text{CN})_2]^+$  does not exhibit any strong absorption in the region 370–730 nm. The photo-generated  $[\text{Pt}(\text{dtbipy})(\text{CN})_2]^+$  species is tentatively assigned as a platinum(III) species.<sup>9</sup>

Reductive quenching of  $[\text{Pt}(\text{dtbipy})(\text{CN})_2]^+$  by  $N,N,N',N'$ -tetramethyl-*p*-phenylenediamine (tmpd) has also been found. The measured quenching rate constant is  $1.78 \times 10^{10}$   $\text{dm}^3 \text{mol}^{-1} \text{s}^{-1}$ , suggesting that the photochemical reaction is essentially diffusion controlled. The transient difference absorption spectrum recorded 10  $\mu\text{s}$  after flashing a degassed acetonitrile solution of  $[\text{Pt}(\text{dtbipy})(\text{CN})_2]$  and tmpd revealed the presence of the  $\text{tmpd}^+$  intermediate ( $\lambda_{\text{max}}$  at 560 and 605 nm).<sup>11–13</sup> Thus the quenching reaction is electron transfer in nature, as represented by equation (5).



In order to justify the estimation of the excited-state redox potential, a comparison has been made between the value

**Table 1** Rate constants for the reductive quenching of  $^3[\text{Pt}(\text{dtbipy})(\text{CN})_2]^*$  by organic donors in dichloromethane at  $20 \pm 0.2^\circ\text{C}$ 

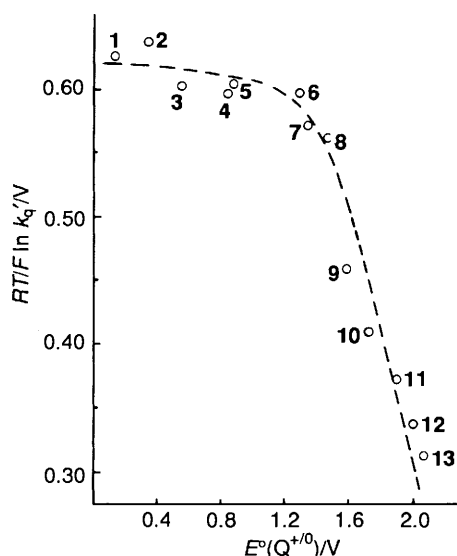
| Organic donor   | $k_q/\text{dm}^3 \text{ mol}^{-1} \text{ s}^{-1}$ | $k_q^a/\text{dm}^3 \text{ mol}^{-1} \text{ s}^{-1}$ |
|---|---|---|
| 1 <i>N,N,N',N'</i> -Tetramethyl- <i>p</i> -phenylenediamine | $1.46 \times 10^{10}$                             | $5.41 \times 10^{10}$                               |
| 2 <i>N,N,N',N'</i> -Dimethylbenzidine                       | $1.63 \times 10^{10}$                             | $8.81 \times 10^{10}$                               |
| 3 Phenothiazine   | $1.06 \times 10^{10}$                             | $2.26 \times 10^{10}$                               |
| 4 Diphenylamine   | $9.36 \times 10^9$                                | $1.76 \times 10^{10}$                               |
| 5 Triphenylamine  | $1.11 \times 10^{10}$                             | $2.49 \times 10^{10}$                               |
| 6 Aniline   | $9.42 \times 10^9$                                | $1.78 \times 10^{10}$                               |
| 7 1,4-Dimethoxybenzene                                      | $5.36 \times 10^9$                                | $7.32 \times 10^9$                                  |
| 8 1,2-Dimethoxybenzene                                      | $3.57 \times 10^9$                                | $4.35 \times 10^9$                                  |
| 9 Hexamethylbenzene   | $7.91 \times 10^7$                                | $7.94 \times 10^7$                                  |
| 10 Pentamethylbenzene                                       | $1.03 \times 10^7$                                | $1.03 \times 10^7$                                  |
| 11 1,2,4-Trimethylbenzene                                   | $2.47 \times 10^6$                                | $2.47 \times 10^6$                                  |
| 12 1,2,3-Trimethylbenzene                                   | $6.41 \times 10^5$                                | $6.41 \times 10^5$                                  |
| 13 1,4-Dimethylbenzene                                      | $2.21 \times 10^5$                                | $2.21 \times 10^5$                                  |

<sup>a</sup> The quenching rate constants  $k_q^a$  have been corrected for diffusional effects using the diffusion-limited rate constant  $2 \times 10^{10} \text{ dm}^3 \text{ mol}^{-1} \text{ s}^{-1}$ .

**Table 2** Stern-Volmer quenching rate constants for the quenching of  $^3[\text{Pt}(\text{dtbipy})(\text{CN})_2]^*$  by hydrogen-atom donors in dichloromethane at  $20 \pm 0.2^\circ\text{C}$ 

| Substrate                              | $k_q^a/\text{dm}^3 \text{ mol}^{-1} \text{ s}^{-1}$ |
|--|---|
| Cyclohexene                            | $6.60 \times 10^7$                                  |
| Cyclooctene                            | $2.66 \times 10^8$                                  |
| Cycloheptene                           | $1.29 \times 10^8$                                  |
| Cyclopentene                           | $1.67 \times 10^8$                                  |
| $[\text{}^2\text{H}_{10}]$ Cyclohexene | $6.46 \times 10^7$                                  |
|  | ( $k_H/k_D = 1.02$ )                                |
| Methylbenzene                          | $2.46 \times 10^5$                                  |
| Ethylbenzene                           | $1.80 \times 10^5$                                  |

<sup>a</sup> Emission lifetimes monitored at 485 nm.

**Fig. 7** Plot of  $RT/F \ln k_q'$  against  $E^0(\text{Q}^{+/0})$  in V vs. saturated calomel electrode

calculated from thermodynamic considerations and that determined through quenching studies with a series of aromatic hydrocarbons in dichloromethane. This class of aromatic hydrocarbons (Table 1) have similar size and electronic structure but different  $E^0$ . For each quencher the Stern-Volmer plot is linear over the range of quencher concentrations. The measured quenching rate constants  $k_q$  as well as the rate constants  $k_q^a$  corrected for diffusional effects are in Table 1.

Based on the kinetic scheme proposed by Rehm and Weller<sup>14,15</sup> and using the theoretical treatment by Marcus,<sup>16,17</sup> a plot of  $RT/F \ln k_q'$  versus  $E^0(\text{Q}^{+/0})$  ( $\text{Q} = \text{quencher}$ ) should give a line with slope of 0.5 in the region where  $|\Delta G_{23}| \ll 2$ . Fig. 7 shows the plot of the quenching rate data. The measured slope is 0.52, in good agreement with the theoretical value. This suggests that the quenching reaction is outer-sphere electron transfer in nature. From the plot, the excited-state potential  $E^0(\text{Pt}^*-\text{Pt}^{\text{I}})$  is 2.14 V vs. normal hydrogen electrode,<sup>18</sup> which is quite close to that of 2.1 V calculated on thermodynamic grounds.

To evaluate the potential of this platinum complex in photoinduced hydrogen-atom abstraction, the quenching of  $[\text{Pt}(\text{dtbipy})(\text{CN})_2]^*$  by a series of hydrogen-atom donors has been investigated and the results are listed in Table 2. The unexpected high quenching rates for cycloalkenes cannot be attributed to an energy-transfer process because the triplet energies of these cycloalkenes are too high for energy transfer to occur. However, H-atom abstraction via the intermediate  $[\{\text{Pt}(\text{dtbipy})(\text{CN})_2\}]_2 \cdots \text{HR}$  ( $\text{R} = \text{cycloalkenyl}$ ) is unlikely to be responsible for the quenching pathway because virtually no kinetic isotope effect has been found for the quenching by cyclohexene ( $k_H/k_D = 1.02$ ). Furthermore broad-band irradiation of an acetonitrile solution of  $[\text{Pt}(\text{dtbipy})(\text{CN})_2]$  and cyclohexene for 10 h showed no coupling products from cyclohexyl radicals. We believe that the quenching of  $[\text{Pt}(\text{dtbipy})(\text{CN})_2]^*$  by cycloalkenes may be attributed to diradical formation, as is found in the photochemistry of  $[\text{Pt}_2(\text{P}_2\text{O}_5\text{H}_2)_4]^{4-}$ .<sup>19</sup>

### Acknowledgements

We acknowledge financial support from the Croucher Foundation and University of Hong Kong. K. T. W. acknowledges the receipt of a Croucher Foundation Studentship, administered by the Croucher Foundation.

### References

- 1 C. M. Che, L. Y. He, C. K. Poon and T. C. W. Mak, *Inorg. Chem.*, 1989, **28**, 3081.
- 2 (a) V. M. Miskowski and V. H. Houlding, *Inorg. Chem.*, 1989, **28**, 1529; (b) H. Kunkely and A. Vogler, *J. Am. Chem. Soc.*, 1990, **112**, 5625.
- 3 (a) G. M. Bager and W. H. F. Sasse, *J. Chem. Soc.*, 1956, 616; (b) A. Avshu and A. W. Parkins, *J. Chem. Res.*, 1984, (S) 245.
- 4 C. M. Flynn and J. N. Demas, *J. Am. Chem. Soc.*, 1974, **96**, 1959.
- 5 M. K. DeArmond, C. M. Carlin and W. L. Huang, *Inorg. Chem.*, 1980, **19**, 62.
- 6 G. L. Geoffroy, M. S. Wrighton, G. S. Hammond and H. B. Gray, *J. Am. Chem. Soc.*, 1974, **96**, 3105.
- 7 H. B. Gray, *Transition Met. Chem.*, 1965, **1**, 239.
- 8 M. Chou, C. Creutz, D. Mahajan, N. Sutin and A. P. Zipp, *Inorg. Chem.*, 1982, **21**, 3989.
- 9 C. M. Che, K. T. Wan, L. Y. He, C. K. Poon and V. W. W. Yam, *J. Chem. Soc., Chem. Commun.*, 1989, 943.
- 10 K. B. Yoon and J. K. Kochi, *J. Am. Chem. Soc.*, 1988, **110**, 6586.
- 11 S. J. Milder, R. A. Goldbeck, D. S. Kliger and H. B. Gray, *J. Am. Chem. Soc.*, 1980, **102**, 6761.
- 12 A. C. Albrecht and W. T. Simpson, *J. Am. Chem. Soc.*, 1955, **77**, 4454.
- 13 J. T. Richard and J. K. Thomas, *Trans. Faraday Soc.*, 1970, **66**, 621.
- 14 D. Rehm and A. Weller, *Ber. Bunsenges. Chem.*, 1969, **73**, 834.
- 15 D. Rehm and A. Weller, *Isr. J. Chem.*, 1970, **8**, 259.
- 16 R. A. Marcus, *J. Chem. Phys.*, 1968, **43**, 679.
- 17 R. A. Marcus, *J. Chem. Phys.*, 1956, **24**, 966.
- 18 C. R. Bock, J. A. Connor, A. R. Gutierrez, T. J. Meyer, D. G. Whitten, B. P. Sullivan and J. K. Nagle, *J. Am. Chem. Soc.*, 1979, **101**, 4815.
- 19 D. M. Roundhill, H. B. Gray and C. M. Che, *Acc. Chem. Res.*, 1989, **22**, 55.

Received 25th July 1990; Paper 0/03390A